Load Sharing in Gravel Decked Log Stringer Bridges

C. Kevin Lyons
Matthew Lansdowne
D. M. Bennett

ABSTRACT

Log bridges are an economical alternative to steel and concrete structures for temporary crossings; however, reduced availability of large logs for stringers and the advancing age of existing log bridges increases the importance of structural analysis. Load sharing between the stringers is complicated and can result from load spread due to the gravel deck, cable lashing, and mechanical interlocking and friction between the stringers. This paper describes the development of a finite element model (FEM) for gravel decked log stringer bridges that includes elements capable of transferring vertical loads between the stringers. The FEM was used to interpret load deflection data from two *in-situ* bridges. The results of this paper suggest the segments of lashing that pass under one stringer and over an adjacent stringer contribute to load sharing between the stringers; however, care must be taken to ensure that the pattern of lashing supports the stringers directly loaded by the live loads.

Keywords: *log bridge, finite element model, structural mechanics, stringers, load sharing*

Introduction

Keller and Sherar (2003) note that log bridges are commonly used in remote areas due to the availability of local materials. Bradley and Pronker (1994) and Aust et al. (2003) have found gravel decked log stringer bridges and timber bridges are an economical alternative to steel bridges for temporary creek crossings; however, the availability of large diameter logs for stringers is decreasing as the forest industry shifts to second-growth timber. Using smaller diameter logs as stringers increases the reliance on sharing the live loads between the stringers in order to meet a particular load rating, and this is difficult to assess through existing structural analysis procedures. Additionally, aging log stringer bridges can fail due to rot, damage due to overloading, or improper design and construction. Often the redundant stringers in log bridges are able to take up the additional load if a particular stringer fails; however, accidents such as reported by WorkSafeBC (2006) can result in fatalities when machines fall off the bridge due to stringer failure.

Design guides such as the *Log Bridge Handbook* (Nagy et al. 1980) either assume full load sharing between the stringers where live loads are evenly distributed between the stringers, or the live loads are distributed to the stringers as a function of the load spread angle of the gravel surface and the gravel depth. For the bridges considered in this paper, load sharing between the log stringers can be a function of the gravel decking, the cable lashing used to bind the stringers together, and mechanical interlocking between the stringer surfaces. Lyons and Lansdowne (2006) demonstrated that it is unlikely that load distribution due to the live loads is uniform at the interface between the gravel decking and the stringers, and this could result in certain stringers receiving significantly more of the live load. Nagy et al. (1980) noted that cable is used to lash the stringers together to share the load between the stringers directly loaded by vehicle traffic and the unloaded stringers; however, the magnitude of this load sharing has not been documented. It is difficult to measure the actual loads being applied to each stringer in a gravel decked log stringer bridge. Ammeson et al. (1988) modeled cable and log structures using matrix methods; these methods are attractive since the model can be run as a macro in Microsoft Excel which is accessible to most forest engineers. This paper uses a finite element model (FEM) to link the live loads applied to a log stringer bridge to measured deflections of the stringers.

As existing log stringer bridges decay over time, it is necessary to take into account the reduction in the area of the log cross sections due to rot when performing bridge inspections (Moody et al. 1979). In addition, the lashing can slacken as a bridge ages and this may affect the load sharing between the log stringers. A FEM for gravel decked log stringer bridges will allow engineers to factor out the rot from the log stringers where it actually occurs in the logs.

The objectives of this paper are:

1. to describe the development of a FEM for gravel decked log stringer bridges that includes elements used to represent load sharing between the stringers and that can be run as a macro in Microsoft Excel to facilitate access for practitioners and
2. to determine if the vertical component of the tension in the cable lashing is contributing to load sharing between the stringers.

The authors are, respectively, Assistant Professor (kevlyons@interchange.ubc. ca), Dept. of Forest Resource Management, Univ. of British Columbia, Vancouver, BC V6T-1Z4; Supervisor – Engineering Services Canada East (matt.lansdowne@ intertek.com), Intertek Testing Services NA Ltd., Coquitlam, BC V3K 7C1; and Group Leader (dbennett@vcr.feric.ca), Forest Engineering Research Institute of Canada, Vancouver BC V6T 1Z4. This paper was received for publication in July 2007.

International Journal of Forest Engineering 19(1): 42-50.

FEM Development

Elements

In this paper an element connects two adjacent nodes. The log stringers in this paper are modeled using three-dimensional beam elements. Each stringer is divided into 40 equal length ele- ments, and the stringer elements are assumed to be sufficiently short so taper can be ignored within the element. It is assumed that the cable lashing transfers only vertical loads in response to differential deflection between adjacent stringers. To model this, the lashing is modeled as a one-dimensional element capable of resisting only differential vertical translation between the element ends. This element is termed a load sharing element (LSE), and has one degree of freedom at each end, for two degrees of freedom per element. The LSE connect adjacent nodes on adjacent stringers.

The equation defining the LSE element is:

$$\begin{bmatrix} F_{Z1} \\ F_{Z2} \end{bmatrix} = \begin{bmatrix} c & -c \\ -c & c \end{bmatrix} \begin{bmatrix} \Delta_{z1} \\ \Delta_{z2} \end{bmatrix} \quad [1]$$

where:

c = the LSE stiffness constant,

F_{Z1} and F_{Z2} = the vertical forces acting on the end nodes of the element, and

Δ_{z1} and Δ_{z2} = the vertical translations of the end nodes of the element.

Loads

Lyons and Lansdowne (2006) constructed a FEM of the gravel surface of a log bridge. They found that the stress field applied to the log stringers due to the wheel loads was relatively insensitive to the size of the tire footprint for standard log truck tires. Therefore, the vertical stress distribution at the interface between the gravel and the stringers can be found for a unit load and this can be multiplied by the load of interest to find the corresponding stress distribution. Lyons and Lansdowne (2006) used a nonlinear least squares fitting routine to fit Equation [**2**] to their FEM results. Equation [**2**] relates the vertical stress (σ) at the gravel and stringer interface to the depth of the gravel (d_g) and the lateral distance from the center of the wheel load (r) for a unit load acting on the tire contact patch.

$$\sigma = a\, d_g^b\, e^{(-c\, d_g^d\, r^2)} \quad [2]$$

Here a, b, c, and d are constants (**Table 1**). The stress along the base of the gravel due to an applied wheel load (σ_L) can be calculated at a point by multiplying σ by the wheel load (W).

$$\sigma_L = a\, d_g^b\, e^{(-c\, d_g^d\, r^2)}\, W \quad [3]$$

As d_g increases the stress distribution given by Equation [**3**] flattens, and from **Figure 1** it can be seen the vertical stress at the base of the gravel approaches zero when $r = 0.5$ m for the d_g found in the measured bridge data considered in this paper. Thus, given the stringer diameters presented, the stress field from one wheel will be applied to a maximum of two to three stringers. Note, in this paper a dual wheel assembly will be modeled as two wheels with separate contact patches on the gravel deck. For a single drive axel with four wheels, this results in four overlapping stress distributions generated by Equation [**3**]. The combined σ_L applied at a given point at the base of the gravel deck is the sum of the stress fields from the wheels applied to the gravel deck.

Table 1. ~ *Coefficients for the unit load data including depth and position (Lyons and Lansdowne 2006).*

Coefficient			
a	*b*	*c*	*d*
0.7839	–1.8002	2.4684	–1.7731

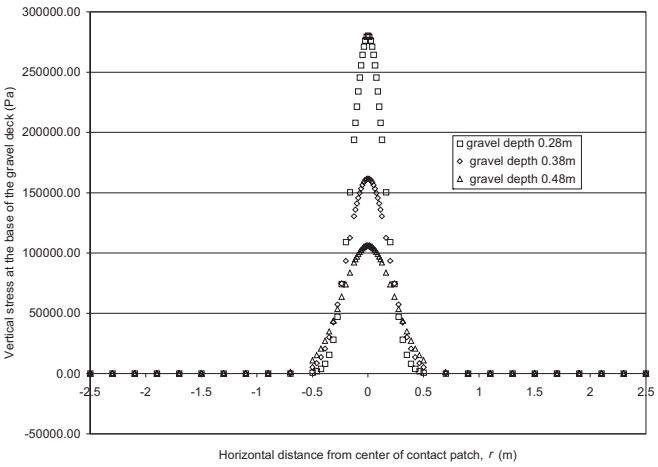

Figure 1. ~ *Stress distribution at the base of the gravel for wheel 3.*

The stress at the base of the gravel surfacing due to the gravel self-weight (σ_D) is calculated from the specific weight and depth of the gravel surfacing assuming a constant surfacing thickness over the span of the bridge.

$$\sigma_D = \gamma d_g \quad [4]$$

Here γ is the specific weight of the gravel. The total vertical stress at the base of the gravel surfacing (σ_T) is the combination of the stress from the live loads, and the stress from the gravel self-weight.

$$\sigma_T = \sigma_L + \sigma_D \quad [5]$$

The total stress σ_T is used to generate loads applied to the stringer nodes resulting from the live loads and the self-weight of the gravel. The base of the gravel is discretized into main rectangles centered on the stringer nodes. To convert the stress distribution at the base of the gravel to discrete forces, the stress is calculated for a point and this is multiplied by the area of discrete rectangle. The accuracy of this method of converting a continuous stress field to discrete forces applied at the stringer nodes is dependent on the coarseness of the mesh. Since the

main rectangles are centered on the stringer nodes, increasing the number of nodes per stringer will reduce the coarseness of the mesh; however, since the stringers are a fixed distance apart, the reduction in coarseness is only in the direction of the stringer. The computational cost is small at the load formation stage of the program; therefore, the main rectangles were further divided into 1,600 sub rectangles. For a given main rectangle the average σ_L from the sub rectangles is calculated for each wheel load and the sum of these are added to σ_D to produce σ_T, then σ_T is multiplied by the area of the main rectangle to produce the vertical force applied to the stringer node assigned to the main rectangle.

The stringer elements have constant circular cross sections; therefore, the self-weight is a uniformly distributed load over each element. Equivalent forces and moments at the stringer nodes, due to the stringer self weight, are calculated using methods suggested by Weaver and Gere (1980). The total load applied to a stringer node is the combination of the live loads, the dead load due to the gravel self-weight, and the dead load due to the stringer self-weight.

Boundary Conditions

The boundary conditions are defined for the nodes located at the stringer ends (**Table 2**). The rotation around the X-axis is restrained to ensure the stability of the model. These conditions model the stringer as a simply supported beam as suggested by Bennett et al. (2004) to approximate the conditions experienced by stringers within a gravel decked log stringer bridge.

Modulus of Elasticity and LSE Stiffness

As noted by Bodig and Jayne (1993) the modulus of elasticity (MOE) can be calculated using the flexural formula. In this method MOE is treated as the unknown variable in the flexural formula, with the deflection increment and load increment being the independent variables. In full-size testing of a small sample of log stringers, Lyons and Bennett (2005) found the confidence interval for MOE was 9.7 to 13.5 GPa (df = 8, α = 0.05) for Douglas-fir stringers. These stringers were all from the same location and it is expected that other populations could have values above or below this. Given the relatively large variation that can be expected in MOE and the sensitivity of stringer deflections to this, MOE will be treated as an unknown in this paper.

In this paper it is assumed that the geometry of the stringers is measured without error; therefore, the unknown variables that affect superstructure stiffness are lashing stiffness (*c*) and stringer MOE. The effects of stringer MOE and *c* are coupled through the deflections of the stringers; therefore, it is necessary to calibrate both of these values for a particular bridge loading case. In this paper MOE is assumed to be the same for all of the stringers in a bridge for a particular load case, since the bridges were constructed of a single species, and the logs in a particular bridge were from the same stand. To calibrate MOE and *c*, the FEM was run iteratively varying MOE and *c* until the sum of the squared differences between the calculated incremental deflections and the measured incremental deflections was minimized. Thus, MOE for a particular bridge and *c* are estimated for each load case.

Table 2. ~ *Boundary conditions.*

	Node located x = 0	Node located x = Span
Rotations restrained	X	--
Translations restrained	X, Y, Z	Y, Z

FEM Solution Method

The FEM is written in Visual Basic and run as a macro in Microsoft Excel. The FEM is based on matrix analysis of framed structures as described by Weaver and Gere (1980). This method relates the total loads acting on the bridge to the displacements of the log stringers through the structure stiffness matrix. The stringer and LSE stiffness matrices are combined to produce the global stiffness matrix for the gravel decked log stringer bridge. Once combined, the global stiffness matrix is reordered, systematically moving the unknown displacements to the top of the matrix, and the prescribed displacements to the bottom of the matrix. The ordered structure load matrix, stiffness matrix, and displacement matrix form a system of simultaneous linear equations. This system of linear equations relating the nodal loads to the corresponding degrees of freedom though the global stiffness matrix is solved using a modified factorization method as discussed by Weaver and Gere (1980).

In-Situ Bridge Data

In May 2005, the Forest Engineering Institute of Canada and International Forest Products Limited instrumented and monitored stringer deflections for two gravel decked log stringer bridges. The first bridge was 2 years old, located at Bear Lake, and had nine Douglas-fir (*Pseudotsuga mensziesii*) stringers (**Fig. 2**). It had two sets of cable lashing located approximately at the third points of the 10 m span, stringer butt inside bark diameters ranging from 570 to 800 mm, and a gravel depth of 280 mm (**Fig. 3**). The second bridge was 1 year old, located at Elk

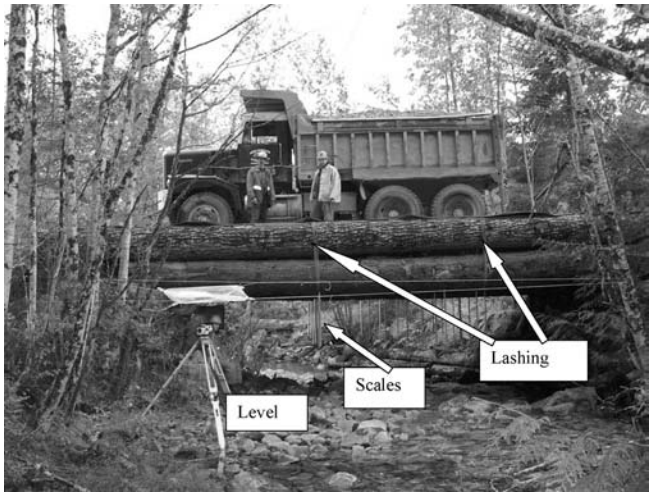

Figure 2. ~ *Bear Lake deflection test setup.*

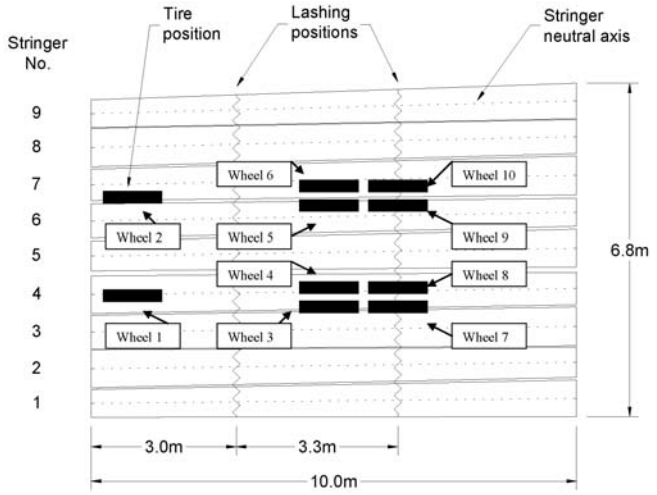

Figure 3. ~ *Plan of Bear Lake bridge center load case.*

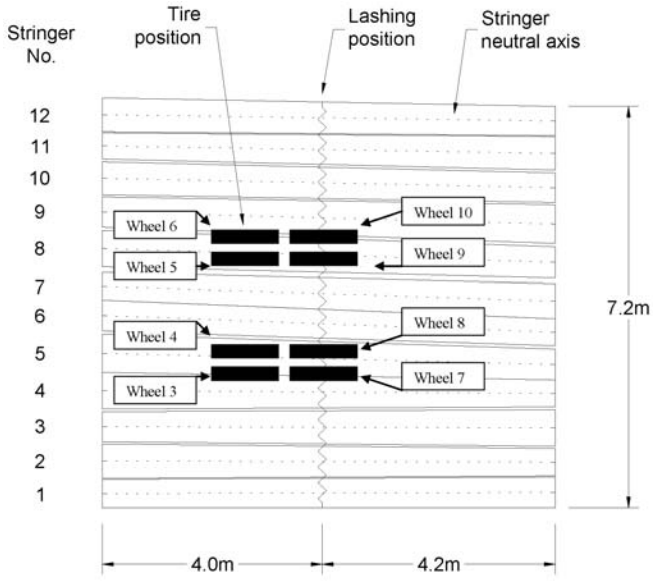

Figure 4. ~ *Plan of Elk Bay bridge center load case.*

Bay, and had 12 Douglas-fir stringers. It had one set of cable lashing located approximately at the mid-point of the 8.2 m span, stringer butt inside bark diameters ranging from 470 to 700 mm, and a gravel depth of 380 mm (**Fig. 4**). The cable lashing for both bridges was 15.9 mm diameter 6 by 19 galvanized independent wire rope core steel cable. The exact Young's modulus of this cable is not know; however, Bridon American Corporation (2006) suggests a range of 87 to 93 GPa.

A three-axle gravel truck was used to load the bridges. The gravel truck had 10 wheels with eight drive wheels located on two drive axles. The wheel loads were measured with portable weight scales and are presented in **Table 3**. Note vehicle position and bridge dimensions limit which wheels fit on the bridge for a given loading configuration. **Figures 3 and 4** provide the wheel numbers for the wheels located on the bridges that correspond to **Table 3**.

Table 3. ~ *Wheel loads.*

Axle	Wheel	Wheel load
		(N)
Steer	1	18973.43
Steer	2	18884.25
Drive 1	3	36163.23
Drive 1	4	36163.23
Drive 1	5	35271.41
Drive 1	6	35271.41
Drive 2	7	38794.09
Drive 2	8	38794.09
Drive 2	9	38860.98
Drive 2	10	38860.98

This study measured deflection of *in-situ* bridges due to vehicle loads; therefore, the at-rest location of the bridge stringers includes deflection due to loading from the weight of the stringers and the gravel decking. The deflection of the bridge stringers due to vehicle loading was measured as follows.

- For the Bear Lake bridge, rulers with 1.0-mm increments were hung on each stringer at the location of the first lashing, mid-span, and the location of the second lashing (**Fig. 2**).
- For the Elk Bay bridge, the rulers were hung on each stringer at the first third of the span, the mid-span lashing point, and the second third of the span.

A high precision level equipped with a micrometer was used to note the ruler scale values that were level with the instrument (Δ_1) prior to loading the bridge with the test truck. The gravel truck was positioned on the bridge and the position was held constant for a given test. With the truck in position on the bridge, the level was used to determine the ruler scale values that were level with the instrument (Δ_2). The difference between Δ_1 and Δ_2 represents the stringer vertical deflection due only to the gravel truck loading (Δ_T), where Δ_T is the incremental deflection of the stringer due to the gravel truck, measured at the point of ruler attachment.

For each of the bridges considered in this paper, the truck was positioned so the centerline of the truck was along the centerline of the bridge, offset from the centerline of the bridge to the upstream side of the bridge, and offset to the downstream side of the bridge. The magnitude of the offset was constant for a particular bridge and was determined by the minimum distance (either upstream or downstream) from the bridge centerline to the berm alongside the guard log. The offset of the truck centerline was calculated by subtracting half the drive axle width from the minimum distance between the bridge centerline and the berm. The offset for the Bear Lake and Elk Bay bridges were 1.165 m and 0.87 m, respectively. The position of the wheel loads with respect to the lashing and stringers for the center load case are given in **Figures 3 and 4**.

Load Sharing Through Cable Lashing

This section considers the actual lashing pattern used in the bridges measured in this study. To consider whether the vertical

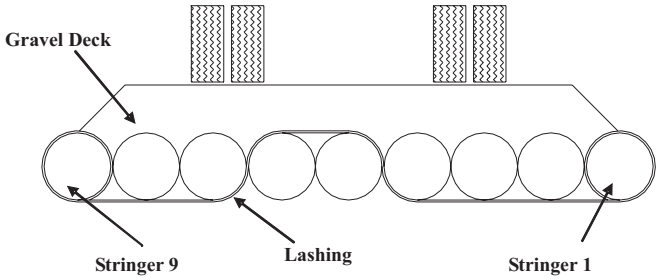

Figure 5. ~ *Lashing diagram for the Bear Lake bridge.*

component of the cable lashing contributes to load sharing between the stringers, it is necessary to examine the pattern of lashing used. In **Figure 5**, it can be seen that the Bear Lake bridge lashing goes around the outside and under stringer 1, under stringers 2 to 4, over the top of stringers 5 and 6, and back under stringers 7 to 9. In general, the truck wheels do not travel directly over stringers 1 and 9. For stringers 2, 3, and 8, the tension in the lashing is acting mostly in the horizontal direction; therefore, to realize a vertical transfer of load through lashing tension, there would have to be significant differential deflection between these stringers and the stringers with the lashing riding on top. For stringer 4, the section of lashing riding up over stringer 5 provides a better opportunity for load sharing between stringers 4 and 5 through a vertical component of the tension. A similar opportunity exists between stringers 7 and 6. Since the lashing is riding on top of stringers 5 and 6, it is not possible for a vertical load applied to these stringers to be shared with the adjacent stringers through a vertical component in the tension.

Considering **Figures 6 to 8** it can be seen the maximum measured deflection in the center load case is less than the maximum for the offset load cases. For the center load case, the wheels are located over stringers 4, 6, and 7 and as noted above the lashing is better positioned to support stringers 4 and 7. While for the downstream case the wheels are located mostly over stringers 5, 6, and 8, and for the upstream case the wheels are mostly located over stringers 2, 3, and 5. For the offset load cases the wheels are located over stringers that are not well supported by the lashing.

In **Figure 9** it can be seen that the Elk Bay bridge lashing goes over top of stringers 1 and 2, underneath stringers 3 to 5, over top of stringers 6 and 7, back under stringers 8 to 10, and over top of stringers 11 and 12. In general the truck wheels do not travel directly over stringers 1, 2, 11, or 12. For stringers 4 and 9 the tension in the lashing is acting mostly in the horizontal direction. Therefore, to realize a vertical transfer of load through lashing tension, there would have to be significant differential deflection between these stringers and the stringers with the lashing riding on top. For stringers 3, 5, 8, and 10, the sections of lashing riding up over adjacent stringers provides a better opportunity for load sharing with the adjacent stringers through a vertical component of the tension. Since the lashing is riding on top of stringers 6 and 7, it is not possible for a vertical load applied to these stringers to be shared with the adjacent stringers through a vertical component in the tension.

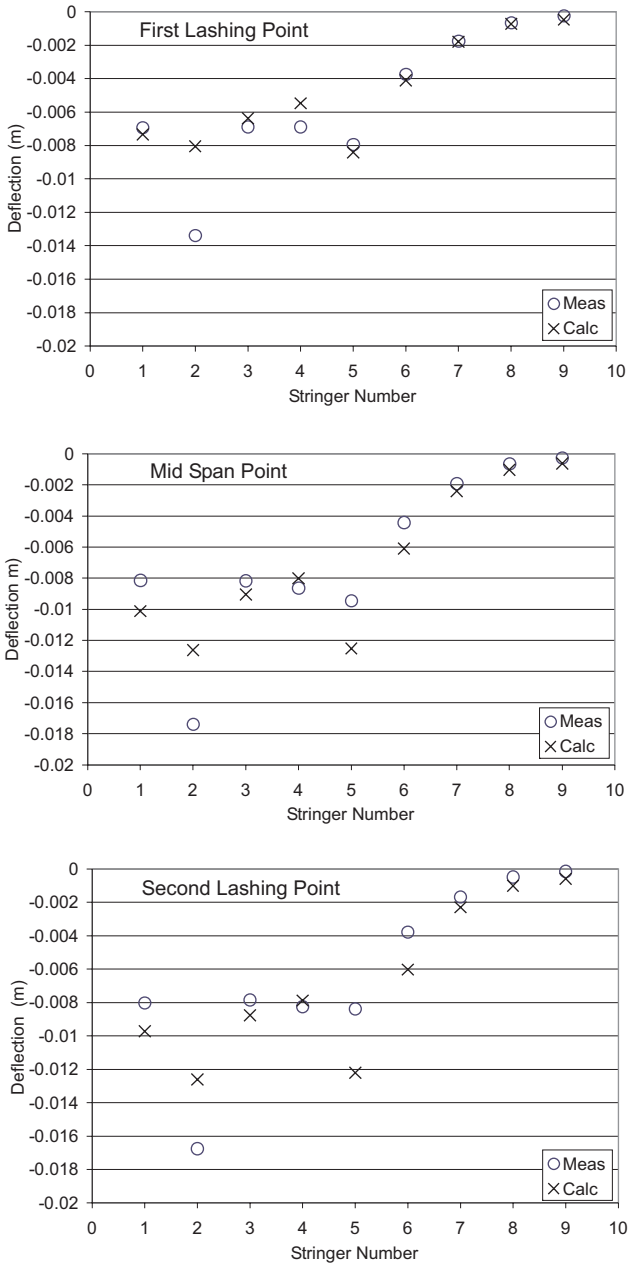

Figure 6. ~ *Bear Lake upstream: measured deflections and calculated deflections using c = 6.22E06 N/m and MOE = 9.6 GPa.*

Considering **Figures 10 to 12**, it can be seen that the maximum measured deflection in the center load case is less than that for the offset load cases. For the center load case, the wheels are located over stringers 5 and 8 and as previously noted the lashing is better positioned to support these stringers. For the downstream case, the wheels are located mostly over stringers 6 and 9, and for the upstream case the wheels are mostly located over stringers 3, 4, and 7. For the offset load cases, the wheels are located over stringers that are not well supported by the lashing.

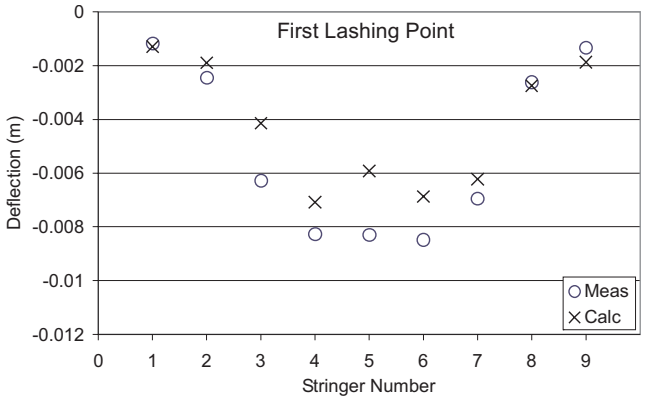

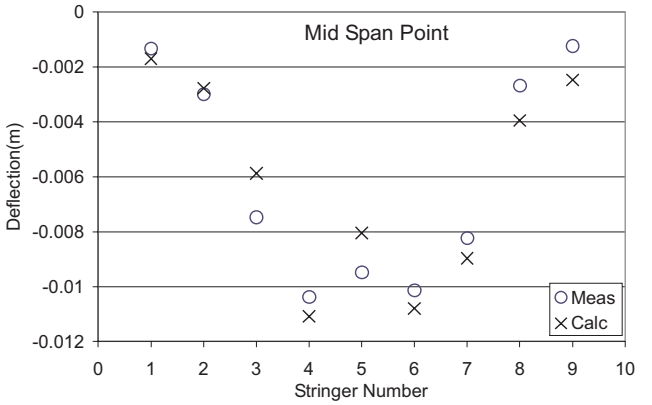

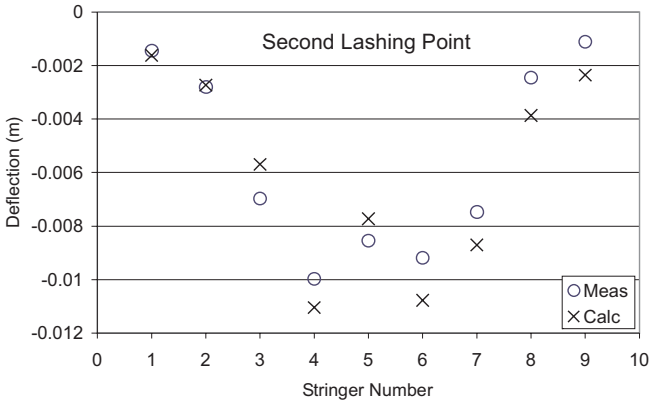

Figure 7. *~ Bear Lake center: measured deflections and calculated deflections using c = 6.79E06 N/m and MOE = 9.7 GPa.*

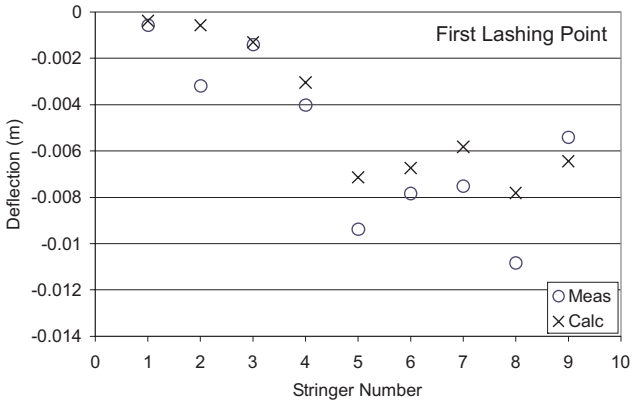

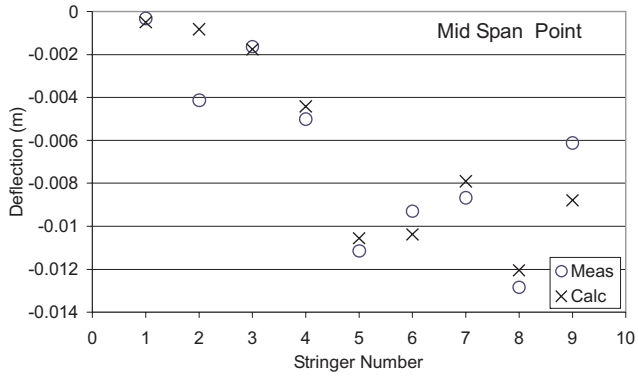

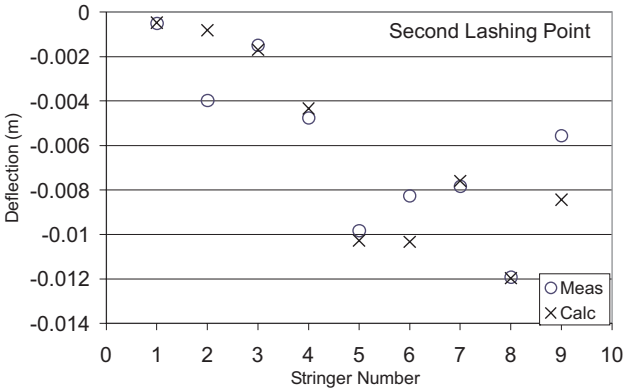

Figure 8. *~ Bear Lake downstream: measured deflections and calculated deflections using c = 6.50E06 N/m and MOE = 9.6 GPa.*

Analysis of LSE Stiffness

The load applied to a stringer due to the differential deflection of a neighboring stringer is a function of the LSE stiffness (*c*). The phenomenon of load sharing between stringers could be a direct component of the cable lashing tension, a function of friction between the surface of the stringers, mechanical interlocking of the stringers due to their irregular shapes, and load spread through the gravel surface. Assuming the algorithm used to model load spread through the gravel is accounting for this mode of load sharing, then *c* is capturing the combined effect of the other modes of load sharing.

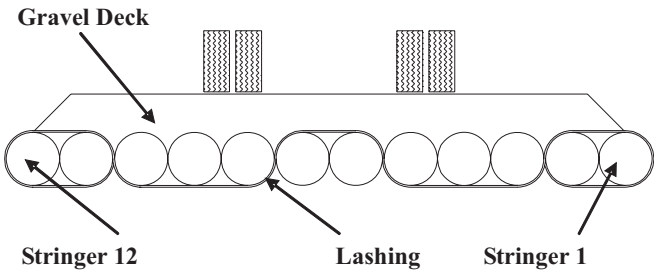

Figure 9. *~ Lashing diagram for the Elk Bay bridge.*

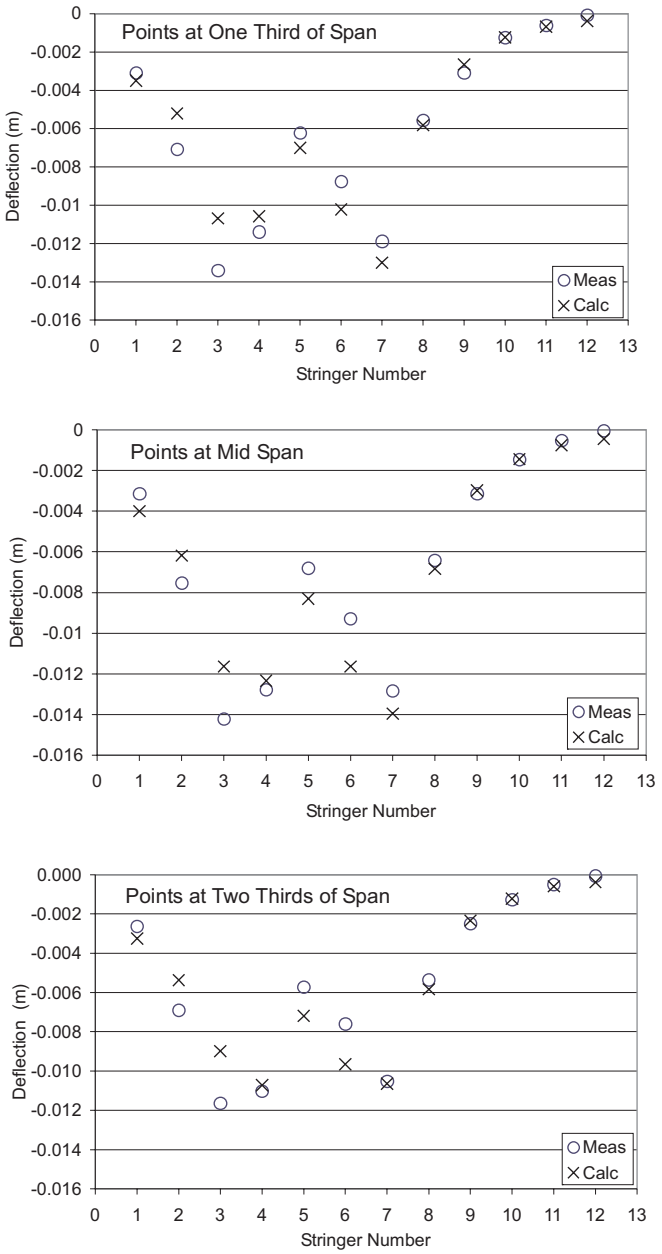

Figure 10. ~ *Elk Bay upstream: measured displacements and calculated displacements using c = 8.48E06 N/m and MOE = 7.9 GPa.*

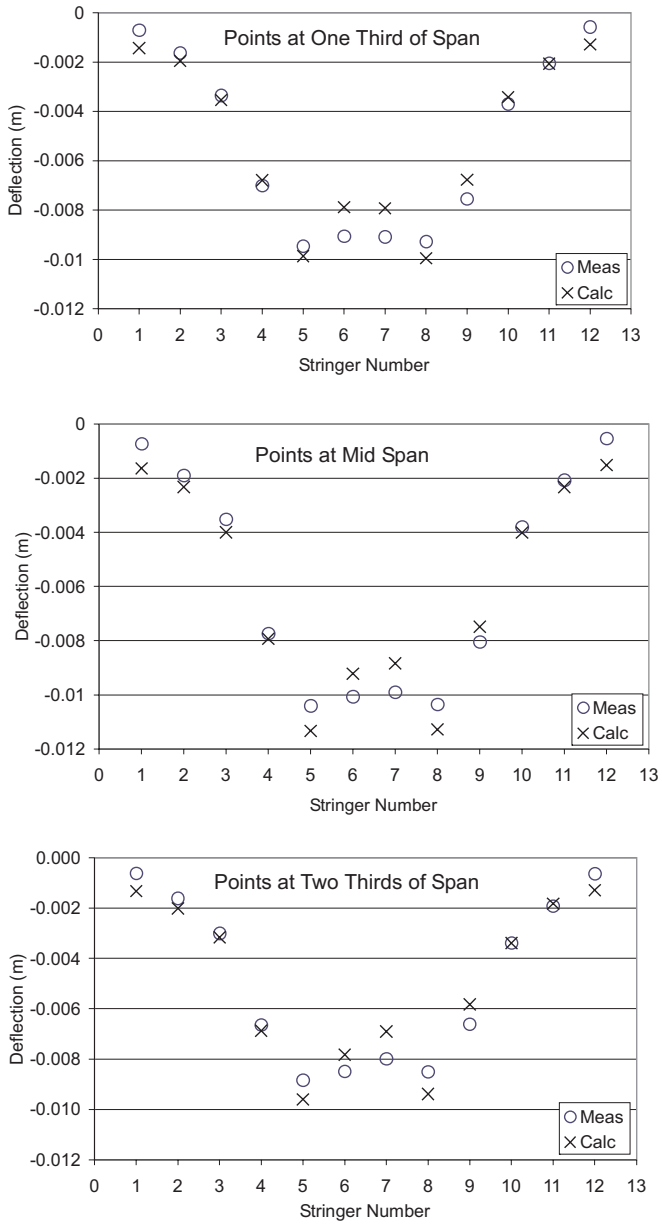

Figure 11. ~ *Elk Bay center: measured displacements and calculated displacements using c = 11.59E06 N/m and MOE = 8.3 GPa.*

Table 4. ~ *Calibrated MOE and LSE stiffness (c) by load case.*

	Downstream		Center		Upstream	
Bridge	c (N/m)	MOE (Pa)	c (N/m)	MOE (Pa)	c (N/m)	MOE (Pa)
Elk Bay	10.18E06	8.3E09	11.59E06	8.3E09	8.48E06	7.9E09
Bear Lake	6.50E06	9.6E09	6.79E06	9.7E09	6.22E06	9.6E09

The *in-situ* bridge data provides six different cases: three load variations for two different bridges. The two bridges considered in this study have different overall dimensions, lashing styles, gravel depths, and number of stringers. Thus, these six cases will give an indication of the variation that can be expected in *c*. MOE and *c* were calibrated for the six cases using the method previously described (**Table 4**). With only one observation per load case for a particular bridge, statistical comparison is not possible; however, the data shows clear trends.

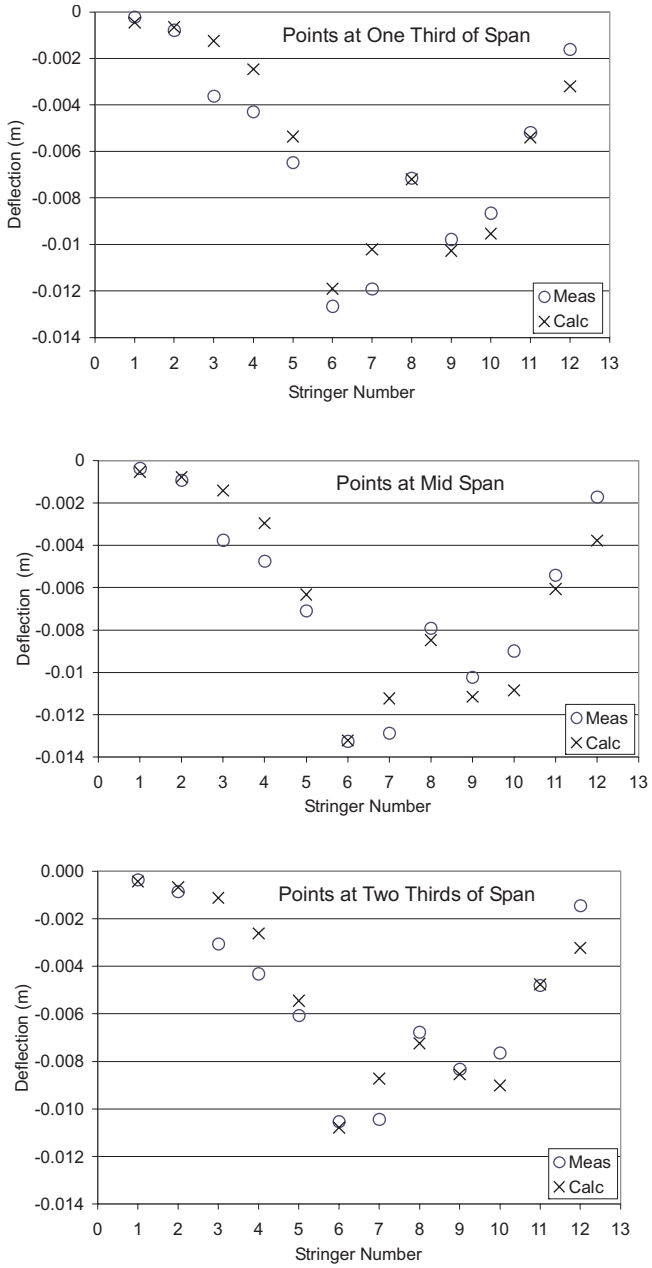

Figure 12. *~ Elk Bay down stream: measured displacements and calculated displacements using c = 10.18E06 N/m and MOE = 8.3 GPa.*

Recall a particular estimate of MOE uses the deflection data from a particular load case on a particular bridge. The range in estimated MOE for a particular bridge is small, 5 percent and 1 percent for Elk Bay and Bear Lake, respectively, when considering the maximum difference as a percent of the smallest value. The narrow range in estimated MOE for a particular bridge is reasonable given that all of the logs in a particular bridge were the same species and obtained from the same location. Note, as the lateral position of the truck is varied, different groups of stringers are supporting the truck. Since load sharing between the stringers is accounted for by the LSE elements, the narrow range in estimated MOE for a particular bridge indicates the stringers had similar stiffness.

The range in estimated *c* for a particular bridge is larger than the range in estimated MOE, 37 percent and 9 percent for Elk Bay and Bear Lake, respectively, when considering the maximum difference as a percent of the smallest value. As noted, for a particular bridge the ability of the lashing to share loads to adjacent stringers varies depending on the stringers being considered. When the truck was positioned in the center of the bridge, the wheels were located over stringers that were better supported by the lashing; however, for the upstream and downstream offsets the stringers taking most of the load were not well supported by the lashing. Since *c* is a measure of the degree that a particular load case is being shared between the stringers, a wide range in *c* for a particular bridge is expected given the lashing configurations used. In the previous section, it was noted the lashing is better positioned to share the load between stringers when the truck is centered on the bridge, and in **Table 4** it can be seen that *c* is highest for the center load cases. This supports the observation that the cable lashing contributes to load sharing between the stringers; however, it is strongly dependent on the position of the lashing.

The calculated deflections for all of the load cases are presented in **Figures 6 to 8 and 10 to 12**. In general when using the calibrated values for MOE and *c*, the calculated deflection closely follows the measured deflections except for stringer 2 in the Bear Lake upstream load case. It does not appear that there was a measurement error for stringer 2 because it shows a similar large deflection for all three measurement locations in the upstream load case. During the upstream load case, the upstream drive wheels are centered over stringer 2. Therefore, it is reasonable that weakness in this stringer would be visible for the upstream case and not for the other cases. Size is not a contributing factor to the large deflections of stringer 2; however, other possible explanations are a crack in the stringer has gone unnoticed, the lashing could be particularly slack around this stringer, or the MOE for that particular stringer could be much less than for the other stringers.

Conclusions

This paper describes the development of a FEM for gravel decked log stringer bridges that includes LSE between the log stringers that can be run as a macro in Microsoft Excel. The LSE stiffness and MOE for each load case was selected so the sum of squared errors between the calculated and measured deflections was minimized. It was found that the LSE stiffness was more variable than MOE for a particular bridge. This result is reasonable given the similarity in species, source location, and size of the log stringers in a bridge as compared to the variable ability of the cable lashing to contribute to load sharing between particular stringers, due to the pattern of weaving the cables around the stringers.

Considering lashing position, it appears the lashing is unable to support certain stringers, while others have a better opportunity for support. When the truck used to load the bridge was

offset so the poorly supported stringers are directly loaded with the live loads, the maximum measured deflection in the bridge is greater than for the center load case where the stringers are better supported by the vertical component of the lashing tension. In addition, the calibrated values of LSE stiffness were found to be higher for the center load case. This suggests that load sharing was greater for the center load cases, and this is consistent with the observations that the vertical component of the cable lashing is able to contribute to load sharing for certain stringers.

The pattern of lashing found in the bridges considered in this paper indicates improvements are required for the gravel decked log stringer bridge FEM. The load sharing elements accounting for load sharing through the lashing tension should only connect a stringer with the lashing passing underneath it to a stringer where the lashing is riding on top. For these elements it will be necessary to form the stiffness as a function of the distance between the stringer with the lashing passing underneath it to the stringer where the lashing is riding on top.

Acknowledgments

The authors gratefully acknowledge the financial assistance provided by the Province of British Columbia through the Forestry Science Program.

Literature Cited

Aust, W.M., R. Visser, T. Gallagher, and T. Roberts. 2003. Cost of six different stream crossing options in the Appalachian Area. Southern J. of Applied Forestry. 27(1): 66-70.

Ammeson, J.E., M.R. Pyles, and H.I. Laursen. 1988. Three-dimensional analysis of guyed logging spars. Computers and Structures. 26(6): 1095-1099.

Bradley, H.A. and V. Pronker. 1994. Standard Design for Using Railcar Subframes as Superstructures for Temporary Bridges on Forest Roads in British Columbia. FERIC Special Report No. SR – 98. FERIC, Vancouver, BC.

Bennett, D.M., R. Modesto, J. Ewart, R. Jokai, S.P. Parker, and M.L. Clark. 2004. Bending strength and stiffness of Douglas-fir and western hemlock log bridge stringers. FERIC Advantage Report 5(42). FERIC, Vancouver, BC.

Bridon American Corporation. 2006. Products 6x19 class [online]. Available from www.bridonamerican.com. Accessed 7 Dec. 2006.

Bodig, J. and B.A. Jayne. 1993. Mechanics of Wood and Wood Composites. Krieger Publishing Co., FL.

Keller, G. and J. Sherar. 2003. Low volume roads engineering best practices management field guide. U.S. Agency for International Development.

Lyons, C.K. and D.M. Bennett. 2005. The effect of taper on the MOE of log stringers. J. of Wood Sci. and Techn. 39(7): 560-568.

Lyons, C.K. and M. Lansdowne. 2006. Vertical stress in the gravel decking of log bridges. Western J. of Applied Forestry. 21(2): 61-67.

Moody, C.R., L.R. Tuomi, E.W. Eslyn, and W.F. Muchmore. 1979. Strength of log bridge stringers after several year's use in southeast Alaska. USDA Forest Service, Forest Prod. Lab., Res. Paper FPL 346, Madison, WI.

Nagy, M., J.T. Trebett, and G.V. Wellburn. 1980. Log Bridge Construction Handbook: 1980. FERIC Handbook No. 3. FERIC, Vancouver, BC.

Weaver, W. and J.M. Gere. 1980 Matrix Analysis of Framed Structures, 2nd ed.Van Nostrand Reinhold, Scarborough, CA.

WorkSafeBC. 2006. Poster #94-26 Check bridge safety [online]. Available from www2.worksafebc.com/i/posters/1994/ fatal9426.html. Accessed 7 Dec. 2006.